Unusual stability of fcc Co(110)/Cu(110)

G. R. Harp, R. F. C. Farrow, D. Weller, T. A. Rabedeau, and R. F. Marks
IBM Almaden Research Center, 650 Harry Road, San Jose, California 95120-6099
(Received 23 July 1993)

It is found that thick (1000 Å) films of fcc Co can be stabilized via epitaxial growth onto Cu(110) substrates at room temperature. These metastable films transform into polycrystalline films of the stable hcp phase if annealed to temperatures above 200 °C. The unusual stability of the fcc phase in the (110) growth direction is linked with the fact that the phase transformation to hcp involves a major disruption of the crystal structure, compared with, e.g., growth of fcc Co on Cu(111). The stabilization of single-crystal fcc Co at room temperature has enabled measurements of the room temperature magnetic properties in these films, for comparison with hcp Co.

I. INTRODUCTION

Epitaxial growth of crystalline materials has been a very successful approach to understanding various electronic properties in a variety of systems. The key to this approach is that the valence level electronic structure is dominated by crystal structural effects, i.e., band structure. Epitaxial growth allows measurements to be made for a given material in different crystalline orientations or even different crystal structures. These measurements may then be compared with the results of band structure calculations, which generally predict a strong dependence of electronic structure on crystal orientation/structure.

This same approach may be applied to the understanding of magnetic properties, since these are also closely linked with crystal structure, especially in itinerant ferromagnets such as Co. For example, most magnetic materials display a magnetocrystalline anisotropy, which is a preferential alignment of the magnetization along some particular crystallographic direction in the material.

As part of this kind of crystal orientation/structure dependent study of the magnetic properties of Co, we explore the growth properties of Co/Cu(110). Although the room temperature stable phase of Co is hexagonal close packed (hcp), by deposition onto a face centered cubic (fcc) crystal such as Cu(110), we find that it is possible to stabilize fcc Co for films >1000 Å thick. This is unusually thick for such a metastable film, and may be compared with, e.g., the stability of fcc Fe/Cu(100), which is stable to approximately 25 Å,[1] or fcc Co/Cu(111), which begins to undergo a phase transition after only 4 Å.[2] These latter examples are much more the rule for thicknesses attainable by epitaxy of metastable crystal structures. There is only one other comparable system where thicknesses approaching 1000 Å can be obtained, that being the bcc Co/GaAs(110) as discovered by Prinz.[3] In the present study we employ low energy electron diffraction (LEED), reflection high energy electron diffraction (RHEED), x-ray diffraction, and angle-resolved x-ray photoelectron diffraction (XPD) as means of structural characterization, and the magneto-optical Kerr effect (MOKE) for magnetic characterization.

II. EXPERIMENT

All the films were prepared in a VG-80M system with a base pressure of 4×10^{-11} mbar. Electron gun sources were used for the deposition of Pt and Co films, and an effusion cell was used for the deposition of Cu. Growth rates in the range of 0.1–0.25 Å/s were typically used. RHEED measurements were made at various stages during film deposition. LEED and XPD measurements were made in a VG Microlab-II system, which also has a base pressure below 1×10^{-10} mbar. Samples are transferred from the deposition chamber to the ESCA-lab in ultrahigh vacuum ($< 10^{-10}$ mbar).

The preparation of Co(110) films began with $SrTiO_3$(110) wafers (Marketech Inc.), typically 1 in. diameters, which were first etched in a solution of $HF:HNO_3:H_2O$ (1:10:10) for about 15 s, and then in $H_2O_2:NH_3OH:H_2O$ (1:1:100) for a few minutes, rinsed in deionized water, and then quickly mounted and loaded into the deposition chamber. The sample was heat-cleaned at 600 °C for ≈20 min, and then 30 Å of Pt was deposited at 600 °C. The Pt grows with a [110] growth axis, but LEED and scanning electron microscopy show evidence of faceting[4] to expose (111) faces.

Onto this surface, 20 Å Co and 100 Å Cu were then deposited at 100 °C. The resulting surface appeared to have the usual (110) type LEED and RHEED patterns, but with a relatively high diffuse background, indicating a rough surface. The films were then annealed to 500 °C, resulting in sharper LEED and RHEED patterns with lower backgrounds. This approach of low temperature deposition followed by high temperature annealing avoids the gross surface faceting which occurs with higher temperature growth,[4] however some residual surface roughness may remain. Finally, Co films were deposited at temperatures between 20 and 100 °C with varying thicknesses. For films >50 Å thick, x-ray photoelectron spectroscopy performed immediately after deposition showed the presence of only Co at the surface, indicating the absence of long-range interdiffusion between Co and Cu.

Two 1000-Å-thick hcp Co samples used for comparison with the Co(110) film were fabricated in the same

0163-1829/93/48(23)/17538(7)/$06.00

deposition system. A Co(0001) film was deposited onto 500 Å Cu(111) at 100 °C/20 Å Co at 100 °C/ 30 ÅPt at 600 °, following the procedures in Ref. 5. A Co(11$\bar{2}$0) film was deposited onto 100 Å CoF/100 Å Fe on a 1-in. GaAs(100) wafer. The GaAs(100) surface (Laser Diode) was first prepared by etching it in a solution of H_2O_2:NH_3OH:H_2O (1:1:100) for a few minutes, rinsing it in deionized water, and then quickly loading it into the deposition chamber. The sample was heat-cleaned to ≈580 °C until a good RHEED pattern was obtained showing sharp streaks with low diffuse background. The Fe seed layer was deposited at 180 °C, and then annealed to 450 °C, and showed excellent ordering in LEED and RHEED, although weak superstructure features were visible in the LEED pattern which could possibly be due to surface segregation of As.[6] Onto this surface, 100 Å of CoFe was deposited at 100 °C, followed by 1000 Å Co at 100 °C. The Co(11$\bar{2}$0) surface has a twofold in-plane symmetry, so the Co film grew in two domains on the fourfold Fe(100) surface, oriented 90° apart in azimuth. The LEED pattern of the Co film was easily identifiable as resulting from the superposition of two domains of a twofold surface. The growth axis was confirmed *ex situ* using x-ray diffraction. This method for the production of Co(11$\bar{2}$0) is based on the similar epitaxial system of Co/Cr(100).[7]

XPD measurements were made using Al $K\alpha$ incident X radiation, except for the data in Figs. 5(b) and 5(c), where Mg $K\alpha$ was used. There is a fixed angle of 55° between the incident x rays and the electron detection direction, and the sample is rotated before the detector to collect intensities as a function of polar angle (measured from the sample normal). The XPD measurements were taken from the Cu $2p_{\frac{3}{2}}$ photoemission line (553 eV), the Co $2p$ photoemission line (including $\frac{3}{2}$ and $\frac{1}{2}$ components, at about 476 eV with Mg $K\alpha$ x rays), the Co LMM Auger emission line (652 eV), or Co LVV Auger emission line (776 eV). XPD intensities as a function of polar angle correspond to the energy-integrated intensity under a photoemission peak after the subtraction of a linear background. This signal is then normalized to the total electron intensity at another kinetic energy where there is no photoemission peak.

Two-dimensional photoelectron diffraction patterns were constructed for Cu(110) and Co(110), from 19 polar angle scans separated by 5° in azimuth (Fig. 5). The polar angle scans representing an irreducible set of data for a given crystal and symmetry are replicated using rotations and mirror operations and are then fed into a routine which interpolates these data onto a square grid of 128×128 points, having a maximum polar angle of 70°. The spacing between grid points represents a constant in the electron momentum parallel to the crystal surface. The grids are then printed using a grayscale intensity algorithm (lighter→higher intensity) and one can imagine looking down onto the surface of a spherical cap when viewing them.

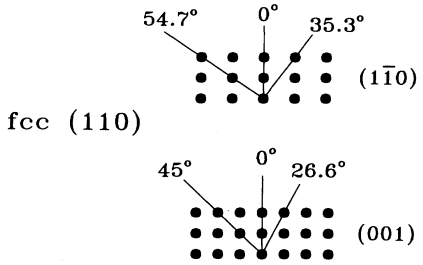

FIG. 1. Diagram of the atom positions near a fcc(110) surface in the [100] and [110] scattering planes.

III. X-RAY PHOTOELECTRON DIFFRACTION

Consider the diagram of atom positions near the fcc(110) surface in Fig. 1, which depicts atoms in (001) and (1$\bar{1}$0) planes perpendicular to the film surface. Note that in the (001) diffraction plane, the two highest density atomic chains in the film are at normal emission (0°) and at 45° polar angles. These atomic chains should therefore give rise to so-called "forward scattering" peaks in the XPD intensity at these same polar and azimuthal angles.[8] Similarly, in the (1$\bar{1}$0) diffraction plane, forward scattering peaks occur at 0° and 55° polar angles. Thus, by measuring the photoelectron intensity as a function of polar angle in these diffraction planes, we can identify a film as having the fcc(110) orientation if it possesses these XPD features.

Data from the XPD intensity of the Cu film substrate (Cu $2p_{\frac{3}{2}}$) are plotted in Fig. 2. These curves plot the normalized XPD intensity of the Cu $2p$ photoemission peak for different Co overlayer thicknesses. Note that this normalization removes the attenuation of the Cu peak intensity caused by the Co overlayer. In the limit of very thin Co films, these data are indistinguishable from the clean Cu substrate. Note that in this regime, the Cu intensity does show strong peaks at normal emission and 45° in the

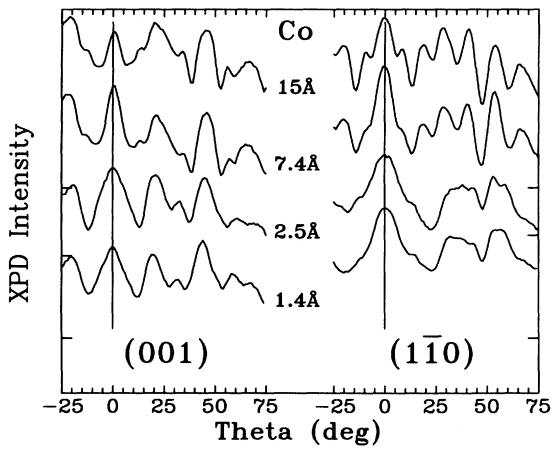

FIG. 2. XPD intensities measured from the Cu(110) substrate $2p$ peak, for various thicknesses of Co overlayer. The lowest Co thickness is indistinguishable from clean Cu. As the Co layer becomes thicker, the positions of the main features do not change, indicating that the Co overlayer is also fcc(110).

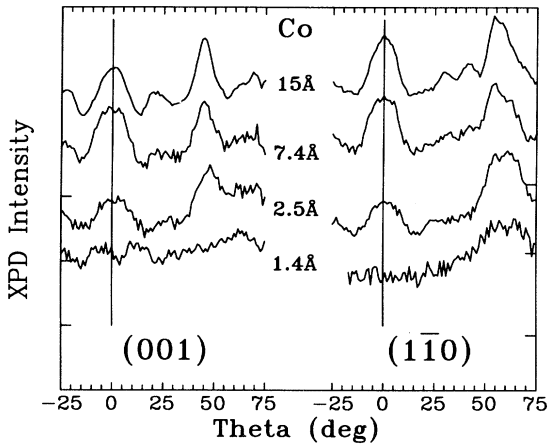

FIG. 3. XPD intensities from thin films of Co on Cu(110), measuring the Co LMM Auger peak. As the Co layer becomes thicker, it presents the same structures as seen in the clean Cu substrate, indicating again that the Co overlayer is in the fcc(110) orientation.

(001) scattering plane, and at normal emission and 55° in the (1$\bar{1}$0) scattering plane, as expected from the forward scattering model. For higher Co layer thicknesses, these peaks do not change position nor disappear (after compensating for the overall attenuation of the buried Cu peak intensity). This is consistent with the conclusion that the Co overlayer is also fcc(110), since if the Co had some other structure, there should result more dramatic changes in the Cu XPD intensity. Some changes in the Cu intensity do occur for thicker Co layers, principally the peaks become sharper and more fine structures appear. This happens because emission from atoms in deeper layers from the surface generally has more fine structure than from near-surface atoms. Because of the Co overlayer, there are no Cu atoms very close to the film surface, and Cu atoms from deeper layers contribute more strongly to the measured XPD.

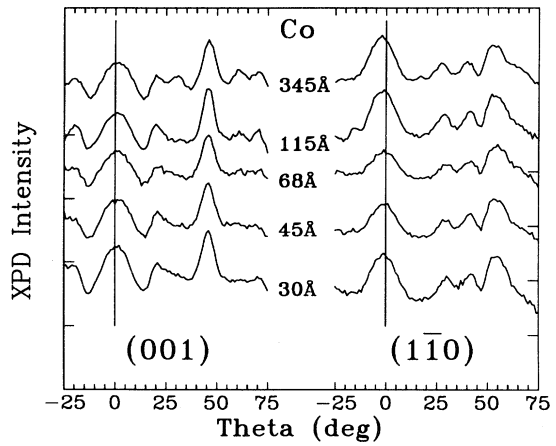

FIG. 4. XPD intensities for thicker films of Co on Cu(110). The features remain unchanged as the film becomes thicker, signifying that Co films up to 350 Å thick are still fcc(110).

Figure 3 displays the analogous data to Fig. 2, except that the XPD intensity is now measured from the Co overlayer (Co LMM). For the thinnest layers, no strong features are present in the XPD intensity since most of

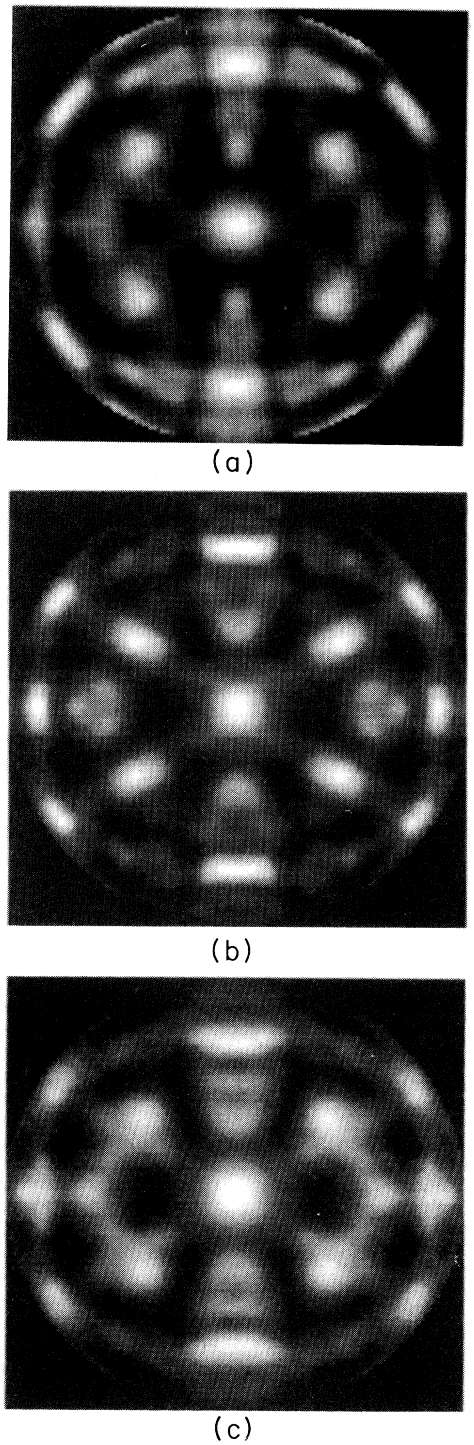

FIG. 5. Two-dimensional diffraction patterns from (a) the $2p$ level of a thick Cu(110) film, (b) the LVV Auger peak of a 1000-Å-thick Co film, and (c) the $2p$ peak from the same Co film. The striking similarity of all three patterns indicates that the Co film is fcc in the (110) orientation.

the Co atoms are on the film surface and do not give rise to forward scattering features. But as the Co films become thicker, clear features emerge in the expected positions for fcc(110). Compare, for example, the spectrum from 15 Å Co/Cu(110) to the spectra from the Cu substrate of Fig. 2. These data unambiguously index this Co film as fcc(110).

Figure 4 show data for thicker Co films (Co *LMM*). Here it is seen that the fcc(110) structure remains stable, up to ≈350 Å thicknesses, indicated by the fact that the XPD structures remain unchanged with increasing Co layer thickness. Note that since 90% of the XPD signal originates from approximately the outer 20 Å of the film, it is not surprising that the XPD features change very little for thicker Co layers, provided the Co films undergo no structural changes.

What is surprising, however, is that the Co films remain in the fcc phase for such thick layers. Recall that fcc Co/Cu(111) and fcc Fe/Cu(100) undergo complete phase transformations at much lower thicknesses. In fact, we find that this fcc phase is stable even for films 1000 Å thick, as demonstrated in Fig. 5. Here we compare the two-dimensional diffraction patterns from a thick Cu(110) film (a) measured with the Cu 2*p* feature, and the diffraction patterns from a 1000-Å-thick Co film measured with (b) the Co *LVV* Auger peak and (c) the Co 2*p* peak. The striking similarity between the Co patterns and the Cu pattern again identifies this Co film as fcc(110). Specifically, the twofold symmetry of the Co XPD patterns is inconsistent with the interpretation that the film is either fcc(111) or hcp(0001), as these orientations would give rise to threefold or sixfold diffraction patterns.

IV. X-RAY DIFFRACTION

X-ray scattering measurements using a rotating anode source were employed to characterize the interior structure of the 1000-Å-thick Co film discussed above. Figure 6 depicts the scattered intensity as a function of momentum transfer q along the film normal. In addition to the substrate and Pt buffer (220) peaks near 4.5 $Å^{-1}$, the Cu(220) and Co(220) peaks appear as a resolved doublet near 5.0 $Å^{-1}$. There is no evidence for other orientations of fcc Co or hcp Co in these data. The Co crystal quality is excellent as indicated by the 100-Å coherence length [Co(220) peak inverse half-width at half maximum (HWHM)] and 1.3° mosaic [Co(220) peak rocking full width at half maximum (FWHM)]. Radial scans through the Cu(200) and Co(200) peaks (inset) confirm the epitaxial relationship of the layers. Analysis of the Co(200) peak yields a 50 Å in-plane correlation length (1/HWHM) and 1.6° in-plane mosaic (FWHM). Finally, the x-ray data demonstrate the Co unit cell is compressed very slightly along the film normal resulting in monoclinic rather than cubic symmetry (i.e., $a = b = 3.549$ Å and $\gamma = 90.37°$).

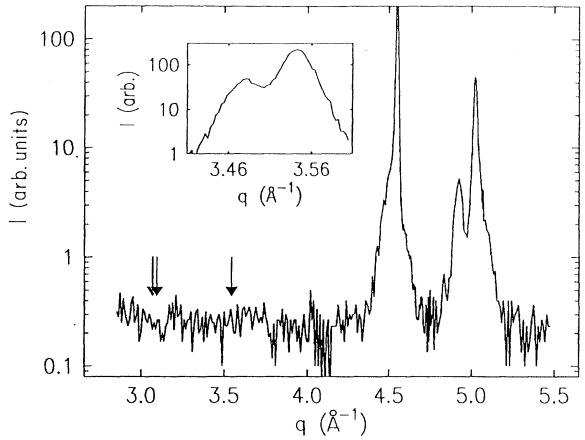

FIG. 6. X-ray specular scattering data for a Co(110) film grown on a Cu(110) seed layer. The Cu(220) and Co(220) peaks are centered at 4.920 $Å^{-1}$ and 5.024 $Å^{-1}$ (respectively) while the strong scattering near 4.5 $Å^{-1}$ stems from the $SrTiO_3$ substrate and Pt seed layer. The arrows denote the expected locations of scattering resulting from Co fcc(111), hcp(0002), and fcc(200) (left to right). The inset depicts an off-specular or asymmetric radial scan through the Cu(200) and Co(200) peaks.

V. LOW ENERGY ELECTRON DIFFRACTION

That the thick Co films deposited at room temperature showed good crystalline quality is further demonstrated in Fig. 7(a). Here we show the LEED pattern at 107 eV taken from a 200-Å-thick Co film. Sharp LEED spots are seen corresponding to the (1,1) and (0,2) re-

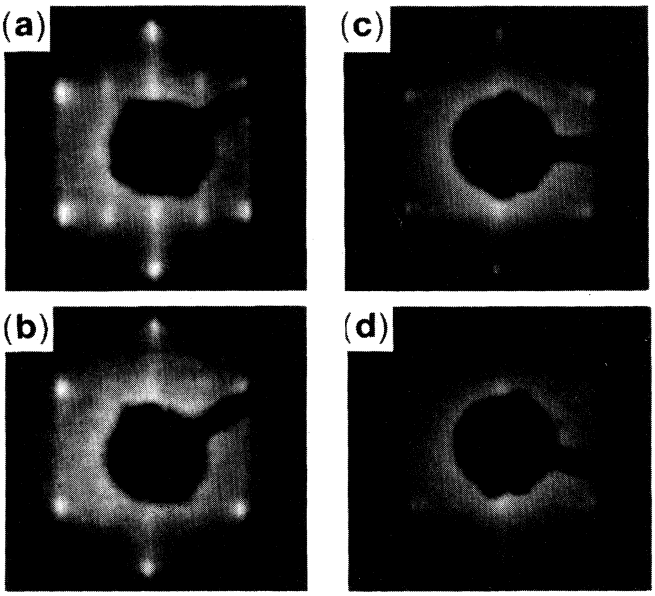

FIG. 7. LEED patterns from a 200-Å film of Co/Cu(110), (a) as grown or after annealing for 10 min to (b) 200 °C, (c) 300 °C, and (d) 400 °C. As grown, the LEED pattern indicates a (110) Co surface with a (2×1) surface reconstruction. With increased annealing, first the reconstruction is lifted while the film progressively degrades to a polycrystalline film of hcp Co.

flections, and weaker, slightly streaked features are seen in the $(\frac{1}{2},1)$ positions. We believe these superstructure features are due to a surface reconstruction of the Co surface because they were seen in most Co films following growth, and no surface contaminant was ever detected by XPS which could account for the superperiodicity.[9] Furthermore, this reconstruction is sensitive to crystalline ordering and is lifted in films with greater disorder (see below).

As a demonstration of the metastability of this Co film, we annealed the film for 10-min intervals to progressively higher temperatures, and then measured the resulting LEED pattern at room temperature. Figure 7(b) shows the result after a 200 °C anneal. The LEED spots are weaker and the diffuse background is higher. This indicates that the film is becoming more disordered, as might occur if the sample were beginning to undergo phase transformation to hcp. Note that the (2×1) superstructure LEED spots have disappeared. This argues against the possibility that the superstructure features might be due to crystalline imperfections in the surface, i.e., the beginnings of the hcp phase transformation, since in the latter case the superstructure should become stronger with annealing.

After a 300 °C anneal, the primary LEED spots appear much weaker, with a still higher diffuse background. After annealing to 400 °C, the LEED spots are almost imperceptible, with nearly all the LEED intensity going into the diffuse background. Note that at 422 °C, hcp Co undergoes a phase transition to the fcc crystal structure. Thus, as the film temperature approaches 422 °C, the energy difference between hcp Co and fcc Co is decreasing, so that the driving force behind the disruption of the present film is *weakening* as the temperature is increased. It is ironic then that this film shows the greatest disorder after the higher temperature anneals. This dilemma is resolved by considering that kinetics also play a role in the phase transformation of the fcc Co films. Higher temperatures also tend to drive the film more quickly toward the energetically favored state. Thus the fcc Co film as grown is in a truly metastable state.

VI. MAGNETIC PROPERTIES

It is well known that bulk hcp Co has a large magnetocrystalline anisotropy, with an easy axis aligned with the [0001] direction (c axis) of the crystal. On the other hand, the high symmetry of the cubic structure in fcc Co gives rise to only very weak magnetocrystalline anisotropy. Magnetic properties can therefore be used as an additional characterization of these films. We present in Fig. 8 three polar Kerr hysteresis loops from three 1000-Å-thick Co films deposited onto various substrates: from an fcc Co(110) film, from an hcp Co(0001) film, and from a (twinned) hcp Co(11$\bar{2}$0) film.

Due to the large demagnetizing field of pure Co, which is $4\pi M_s \simeq 17900$ Oe,[10] all the films presented here have an easy in-plane magnetization direction and the loops in Fig. 8 represent hard-axis loops. For the hcp Co films, the shape of these loops and the saturation fields (the latter

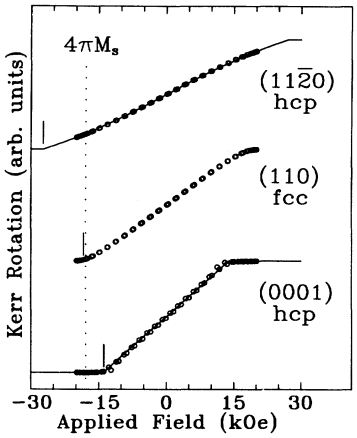

FIG. 8. Polar magneto-optical Kerr loops from hcp Co(11$\bar{2}$0), fcc Co(110), and hcp Co(0001). Here the applied magnetic field is normal to the sample plane. The raw data (every tenth point is plotted with a symbol) are fitted with loop simulations (solid line) to determine the saturation fields (vertical bars). For fit to the Co(11$\bar{2}$0) loop, the saturation Kerr rotation was determined in an independent measurement. The deviation of the saturation fields from $4\pi M_s$ (dotted vertical line) for the two hcp films results from the large magnetocrystalline anisotropy in hcp Co. The saturation field of the fcc Co film is independent of its magnetocrystalline anisotropy in this orientation, and therefore saturates very near to $4\pi M_s$.

marked by vertical bars) contain information about the magnetic anisotropy constants K_1 and K_2, which were evaluated by fitting the loops according to[10]

$$H = \left[4\pi M_s - \frac{2K_1}{M_s}\right]\left(\frac{M}{M_s}\right) - \frac{4K_2}{M_s}\left(\frac{M}{M_s}\right)^3 \quad (1)$$

using $\frac{2K_1}{M_s}$ and $\frac{4K_2}{M_s}$ as fitting parameters. In particular, setting $\frac{M}{M_s} = 1$, the hcp films will saturate in the perpendicular direction at

$$H_{\rm sat} = 4\pi M_s \pm \frac{2K_1}{M_s} \pm \frac{4K_2}{M_s}, \quad (2)$$

where the plus sign is used for the (11$\bar{2}$0) film, and the minus sign for the (0001) film.

In the fcc case, the shape of the loop does not admit such simple analysis and Eq. (1) does not hold. We have determined from in-plane magnetization measurements that the [$\bar{1}$11] direction is the easy axis for this film. Thus, the saturation field of this film in the perpendicular direction is[10]

$$H_{\rm sat} = 4\pi M_s + \frac{2K_1}{3M_s}, \quad (3)$$

where we have assumed K_2 is negligible. The fact that the saturation field of the fcc Co film (18 300 Oe) is very close to $4\pi M_s$ of bulk Co is further evidence of the cubic symmetry of this film (i.e., K_1 is very small). This is especially apparent in comparison with the two hcp Co

films where H_{sat} departs strongly from $4\pi M_s$ due to the reduced symmetry of the hcp crystal structure.[11]

This is a simple example of the kinds of magnetic characterization which can be made now that we have a convenient method for the production of fcc Co films at room temperature. In a future publication,[12] we will consider these issues in more detail, particularly with regard to the absolute value of the saturation Kerr rotation as a function of photon energy. These "Kerr spectra" provide a powerful tool for the probing of the magnetic band structure of such materials.[13]

VII. DISCUSSION

It is known that when Co is deposited on Cu(111), the Co crystal structure begins to transform to hcp(0001) after only 4 Å.[2] This behavior can be understood by considering that both the Co(0001) and Cu(111) have surfaces consisting of a close-packed arrangement of atoms, having lattice constants differing by only ≈2%. This provides a simple mechanism for the phase change from fcc Co to hcp Co, viz., the introduction of stacking faults parallel to the growing film surface. A similar mechanism is the mode of phase transformation in bulk Co crystals,[14] where stacking faults are introduced by slip planes parallel to the (111) directions. In a perfect Co film on Cu(111), such stacking faults introduce dislocations at the lateral boundaries of the film, which therefore cause a negligible addition to the total energy of the system. Moreover, the stacking faults can be built into the film *during growth*, so that there is no activation barrier to the phase transformation from fcc to hcp.

One side effect of this crystal matching between fcc(111) and hcp(0001) is that very high quality single-orientation Co(0001) films may be produced by growth on Cu(111), and this fact has been exploited to produce the Co(0001) film in Fig. 8. In contrast to this, there is no lattice plane in hcp Co analogous to the Cu(110) surface. Thus, when a Co film deposited on Cu(110) transforms to the hcp phase, no long-range epitaxial relationship is retained at the Co/Cu interface. This is demonstrated in Fig. 7, where the hcp Co/Cu(110) film presents a LEED pattern having nearly uniform intensity in all directions, indicating a polycrystalline surface.

This provides a clue as to why Co(110) is so stable on Cu(110). A relatively thin film of fcc Co can be stabilized on Cu(110) because the energy cost paid for being in the metastable fcc phase is compensated by a larger energy cost to create a complex dislocation network at the Co/Cu interface.[15–17] But as the film becomes thicker, the energy paid for maintaining the fcc phase (which scales with thickness) eventually overcomes the interface dislocation energy (a constant). If one requires that the system remain in thermodynamic equilibrium, then the phase transition will occur just at the thickness where these two energies are equal (the critical thickness).

However, the hcp→fcc phase transition in Co is martensitic, i.e., it occurs by the collective motion of large numbers of atoms at a time. The activation energy for such a phase transition can be large. To make an order of magnitude estimate of this activation energy, consider that the fcc→hcp phase transition occurs by the slipping of adjacent {111} planes along a $\langle 11\bar{2} \rangle$ direction, so that if viewed from above the {111} plane, atoms slide from one threefold hollow site, across a bridge site, and into the adjacent threefold hollow. Assuming that the in-plane lattice of the slipping planes is rigid, such a motion induces a volume expansion per interface atom by a factor of $\sqrt{3}/12$ when the atoms cross the bridge sites (assuming hard spheres). First-principles total energy calculations[18] for fcc Co indicate that such a volume change would incur an energy increase of about 0.26 eV/atom. Because the {111} planes meet the (110) surface at a significant angle, and because the Co atoms tend to move collectively, for thin films the activation energy, ΔE, will be proportional to $(\frac{h}{a})0.26$ eV, where h is the film thickness and a is the thickness of a single monolayer. Using a more realistic approach, Bruinsma and Zangwill[17] estimate that ΔE for the bcc→fcc phase transition (also martensitic) in a metastable Co film would be of order $(\frac{h}{a})0.3$ eV.

Such activation energies are significant when compared with room temperature ($kT = 0.025$ eV). Since the nucleation rate for the phase transition is proportional to $\exp(\Delta E/kT)$, if hcp nucleation does not occur when the film is thinnest, it rapidly becomes impossible as h increases. This leads to the counterintuitive result that lower growth temperatures actually *stabilize* the fcc phase. As the temperature decreases, although the fcc→hcp phase transition becomes more favored energetically, the probability of nucleation decreases even more rapidly. Of course if T is increased following growth, the phase transformation will proceed, as seen in the LEED experiment. This type of behavior was predicted in the theoretical study of Bruinsma and Zangwill.[17]

As an additional note, we find fcc Co(110) can also be stabilized on Pt(110), but only to thicknesses of ≈20 Å, after which the structure begins to degrade, eventually degenerating to a polycrystalline film. In this case, the lattice mismatch between Co and Pt (10%) is much poorer than between Co and Cu. This will certainly lead to many dislocations at the Co/Pt interface even while the Co remains in the fcc phase. Thus, when it becomes energetically favorable for Co to transform to hcp, the structure has been significantly weakened, and the transformation proceeds in a straightforward manner.

Finally, there is one other comparable system where unusually thick metastable films are stabilized by epitaxial growth. It was shown by Prinz[3] that bcc Co/GaAs(110) can sometimes be stabilized to films >300 Å thick. We find it suggestive that the two cases which show this remarkable stability are Co in different phases. Moreover, bcc Co was found to be most stable on "rougher" GaAs surfaces. In the present case, it has been established that Cu(110) tends to facet during growth,[4] and although we have attempted to suppress this effect, the Cu(110) starting surface is probably not extremely flat for our samples. Loosely speaking, epitaxy on a rougher surface might lead to greater stability because the film is bonded on "more than one side."

VIII. CONCLUSIONS

We have prepared Co films on Cu(110) in order to determine the maximum thickness at which epitaxial fcc Co(110) may be stabilized before undergoing phase transformation to hcp. The films were characterized using LEED, RHEED, XPD, x-ray diffraction, and Kerr hysteresis loops. We find that this maximum thickness is >1000 Å, in sharp contrast to most other, similar epitaxial systems. We infer from this that the fcc Co(110) is stabilized by two cooperating factors. First, very thin films of Co(110) are stabilized by the energy cost of the large dislocation network which results from total phase transformation. Second, once the film is thick enough to thermodynamically favor the hcp phase, the time constant for this relaxation is already very long (at room temperature) since this phase transformation is martensitic.

We find that thick Co(110) films become unstable for annealing temperatures above 200 °C, where they transform to polycrystalline hcp Co, consistent with the above arguments. Our growth process provides a convenient method for the production of thick fcc Co films at room temperature for studies of the magnetic properties of Co in different crystal structures.

[1] J. Thomassen, B. Feldmann, and M. Wuttig, Surf. Sci. **264**, 406 (1992).

[2] B. P. Tonner, Z.-L. Han, and J. Zhang, Phys. Rev. B (to be published).

[3] G. A. Prinz, Phys. Rev. Lett. **54**, 1051 (1985).

[4] G. R. Harp, R. F. C. Farrow, R. F. Marks, and J. E. Vazquez, J. Cryst. Growth **127**, 627 (1993).

[5] R. F. C. Farrow, G. R. Harp, R. F. Marks, T. A. Rabedeau, M. F. Toney, D. Weller, and S. S. P. Parkin, J. Cryst. Growth (to be published).

[6] K. Sano and T. Miyagawa, Appl. Surf. Sci. **60/61**, 813 (1992).

[7] F. Herman, P. Lambin, and O. Jepsen, Phys. Rev. B **31**, 4394 (1985).

[8] For recent reviews of diffuse electron diffraction, see C. F. Fadley, in *Synchrotron Radiation Research: Advances in Surface Science*, edited by R. Z. Bachrach (Plenum Press, New York, 1990); W. F. Egelhoff, Jr., Crit. Rev. Solid State Mater. Sci. **16**, 213 (1990); S. A. Chambers, Adv. Phys. **40**, 357 (1991).

[9] Note that XPD, which is sensitive to the outer ≈20 Å of the Co film, is not sensitive to the reconstruction of the surface layer seen in LEED.

[10] B. D. Cullity, *Introduction to Magnetic Materials* (Addison Wesley, Reading, 1972), pp. 227 and 228.

[11] Anisotropy constants may be extracted from the loop data of Fig. 8, according to Eq. (1). Setting M_s=1422 kA/m we obtain the values $K_1 = 0.35$ MJ/m^3 and $K_2 = 0.16$ MJ/m^3 for Co(11$\bar{2}$0), and $K_1 = 0.26$ MJ/m^3 and $K_2 = 0.01$ MJ/m^3 for Co(0001). These anisotropy constants should ideally be identical, and equal to those of bulk hcp Co: $K_1 = 0.450$ and $K_2 = 0.15$ MJ/m^3 (Ref. 10). Departures from bulk anisotropy are probably due to structural imperfections present in these films: fcc-like stacking faults in the (0001) film, and grain boundary disorder in the twinned (11$\bar{2}$0) film, both of which are observed in the x-ray diffraction. Following Eq. (3), we find $K_1 = -0.8$ MJ/m^3 for fcc Co.

[12] G. R. Harp and D. Weller (unpublished).

[13] G. R. Harp, D. Weller, T. Rabedeau, R. F. C. Farrow, and M. F. Toney, Phys. Rev. Lett. **71**, 2493 (1993).

[14] Z. Nishiyama, Tohoku Sci. Rep. **25**, 79 (1936).

[15] J. H. Van Der Merwe, J. Appl. Phys. **34**, 123 (1963).

[16] W. A. Jesser and D. Kuhlmann-Wilsdorf, Phys. Status Solidi **19**, 95 (1967).

[17] R. Bruinsma and A. Zangwill, J. Phys. (Paris) **47**, 2055 (1986).

[18] V. L. Moruzzi, P. M. Marcus, K. Schwartz, and P. Mohn, J. Magn. Magn. Mater. **54-57**, 955 (1986).

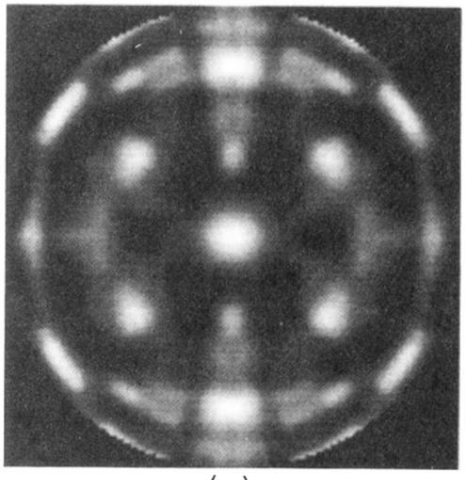

(a)

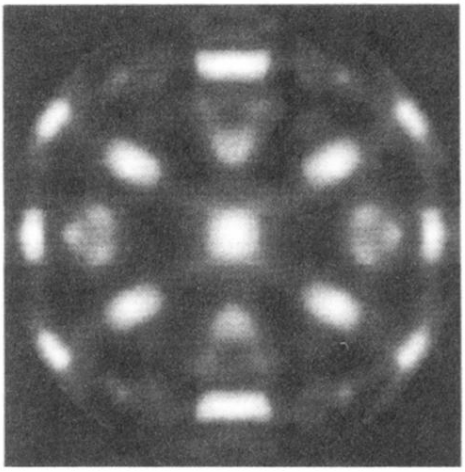

(b)

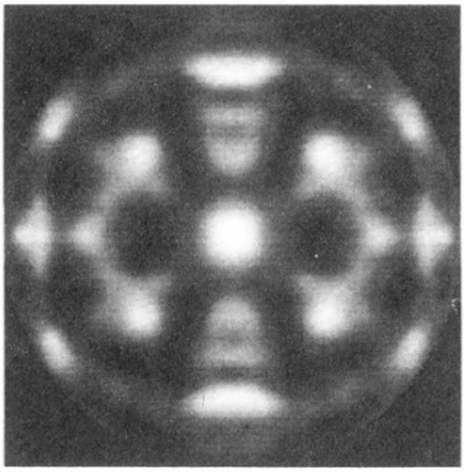

(c)

FIG. 5. Two-dimensional diffraction patterns from (a) the $2p$ level of a thick Cu(110) film, (b) the LVV Auger peak of a 1000-Å-thick Co film, and (c) the $2p$ peak from the same Co film. The striking similarity of all three patterns indicates that the Co film is fcc in the (110) orientation.

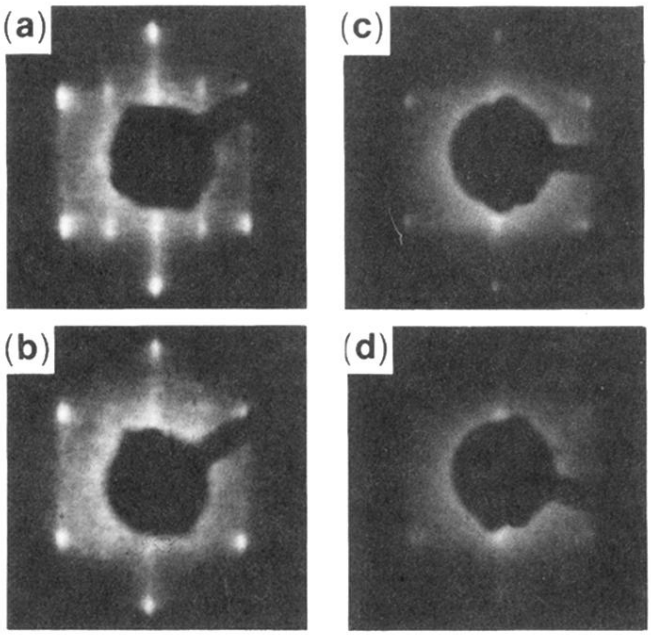

FIG. 7. LEED patterns from a 200-Å film of Co/Cu(110), (a) as grown or after annealing for 10 min to (b) 200 °C, (c) 300 °C, and (d) 400 °C. As grown, the LEED pattern indicates a (110) Co surface with a (2×1) surface reconstruction. With increased annealing, first the reconstruction is lifted while the film progressively degrades to a polycrystalline film of hcp Co.